Polysaccharide BAP1 of *Bifidobacterium adolescentis* CCDM 368 is a biologically active molecule with immunomodulatory properties

Katarzyna Pacyga-Prus [a,*], Dominika Jakubczyk [a], Corine Sandström [b], Dagmar Šrůtková [c], Marcelina Joanna Pyclik [a], Katarzyna Leszczyńska [a], Jarosław Ciekot [d], Agnieszka Razim [a], Martin Schwarzer [c], Sabina Górska [a,*]

[a] *Laboratory of Microbiome Immunobiology, Hirszfeld Institute of Immunology and Experimental Therapy, Polish Academy of Sciences, 53-114 Wroclaw, Poland*
[b] *Department of Molecular Sciences, Swedish University of Agricultural Sciences, Box 7015, SE-750 07 Uppsala, Sweden*
[c] *Laboratory of Gnotobiology, Institute of Microbiology, Czech Academy of Sciences, 549 22 Novy Hradek, Czech Republic*
[d] *Laboratory of Biomedical Chemistry, Hirszfeld Institute of Immunology and Experimental Therapy, Polish Academy of Sciences, 53-114 Wroclaw, Poland*
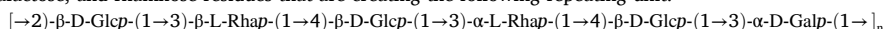
ARTICLE INFO

ABSTRACT

Bifidobacteria are among the most common bacteria used for their probiotic properties and their impact on the maturation and function of the immune system has been well-described. Recently, scientific interest is shifting from live bacteria to defined bacteria-derived biologically active molecules. Their greatest advantage over probiotics is the defined structure and the effect independent of the viability status of the bacteria. Here, we aim to characterize *Bifidobacterium adolescentis* CCDM 368 surface antigens that include polysaccharides (PSs), lipoteichoic acids (LTAs), and peptidoglycan (PG). Among them, Bad368.1 PS was observed to modulate OVA-induced cytokine production in cells isolated from OVA-sensitized mice by increasing the production of Th1-related IFN-γ and inhibition of Th2-related IL-5 and IL-13 cytokines (*in vitro*). Moreover, Bad368.1 PS (BAP1) is efficiently engulfed and transferred between epithelial and dendritic cells. Therefore, we propose that the Bad368.1 PS (BAP1) can be used for the modulation of allergic diseases in humans. Structural studies revealed that Bad368.1 PS has an average molecular mass of approximately $9,99 \times 10^6$ Da and it consists of glucose, galactose, and rhamnose residues creating the following repeating unit:

$$[\rightarrow 2)\text{-}\beta\text{-D-Glc}p\text{-}(1\rightarrow 3)\text{-}\beta\text{-L-Rha}p\text{-}(1\rightarrow 4)\text{-}\beta\text{-D-Glc}p\text{-}(1\rightarrow 3)\text{-}\alpha\text{-L-Rha}p\text{-}(1\rightarrow 4)\text{-}\beta\text{-D-Glc}p\text{-}(1\rightarrow 3)\text{-}\alpha\text{-D-Gal}p\text{-}(1\rightarrow]_n$$

1. Introduction

The definition of probiotics associated with bacterial cell viability has been established over 20 years ago and the promise of applied probiotic bacteria for a variety of health purposes is well-described (Kerry et al., 2018). *Bifidobacterium* strains are Gram-positive, anaerobic bacteria that are constituents of the human microbiota. They play a pivotal role in the immune system maturation and modulation of immune cell responses (Ruiz et al., 2017). Administration of live *Bifidobacterium* strains triggers immune responses either in healthy or allergy-sensitized mice through e.g. changes in cytokine production or specific activation of the immune cells subsets (Hiramatsu et al., 2011; Raftis et al., 2018). Nowadays, it becomes clear that not only live and proliferating bacteria are having a beneficial effect but also certain effector

molecules produced by them (Schiavi et al., 2016; Speciale et al., 2019; Xu et al., 2017). The exopolysaccharides, (lipo)teichoic acids, glycolipids, peptidoglycans, proteins, and other components of probiotic bacteria are of interest as potentially biologically active structures. Recently, they have been named by the International Scientific Association of Probiotics and Prebiotics as "postbiotics" (Nataraj et al., 2020). Health-promoting effects of these molecules are easy to establish through identifiable structures, thus enabling the analysis of structure-function relationships. However, our understanding of the link between a defined postbiotic structure and its biological effect on the host is still in its infancy. Among the most intensively studied bifidobacterial postbiotic molecules are polysaccharides (PSs), peptidoglycans (PGs), and lipoteichoic acids (LTAs).

Bifidobacterial PSs consist mainly of galactoses and glucoses (Inturri

et al., 2017; Nagaoka et al., 1996; Speciale et al., 2019; Zdorovenko et al., 2009). Differences between PSs are based generally on the α/β isomers composition, linkages between monosaccharides, and the order of the sugar residues in a PS chain unit. Bifidobacterial PSs may also contain relatively abundant rhamnose and less frequent mannose or 6-deoxy-D-talose (Altmann et al., 2016; Kohno et al., 2009; Nagaoka et al., 1988; Shang et al., 2013). The biological function of PSs is still not fully explored, but it appears to be strongly related to their chemical structure. The neutral and/or high molecular weight PSs can act as suppressors of the immune responses, while acidic and/or small molecular weight PSs are associated with immunostimulatory properties (Górska et al., 2017; Pyclik et al., 2020; Zhou et al., 2019). PG of the *Bifidobacterium* genus belongs to type A (divided into 4 subtypes A1-A4) and is characterized by the binding of the D-alanine carbonyl group (at the 4th position) and the diamino acid (at the 3rd position) of the neighboring peptide. The primary role of PG is to scaffold bacterial cell and protect against environmental factors. It is also a potent immunomodulator that regulates homeostasis and triggers immune responses by continuous stimulation of NOD receptors (Clarke et al., 2010; Martinic et al., 2017; Wolf & Underhill, 2018). The bifidobacterial LTAs are composed of a hydrophilic backbone (e.g. glycerol-, ribitol-phosphate) and hydrophobic glycolipid anchor creating together an amphiphilic structure, which plays biologically significant roles. Recently, it has been shown that the LTA from *B. animalis* subsp. *lactis* BPL1 reduces fat deposition through the regulation of the IGF-1 pathway in *the Caenorhabditis elegans* model (Balaguer et al., 2022). Moreover, LTA derived from *Lactobacillus reuteri* exhibited anti-inflammatory activity through MAPK and the NF-κβ pathways in LPS-induced macrophages (Lu et al., 2022).

Allergic diseases remain a major public health problem that impacts patients' quality of life (Palomares et al., 2017). Allergic inflammation is typically driven by type 2 immune responses to environmental allergens manifested by the differentiation of naïve T CD4+ cells towards Th2 effector cells, allergen-specific IgE induction, IL-4, IL-5, and IL-13 production, eosinophilia, and mast cells activation. *Bifidobacterium* strains were shown to restore immunological balance and effectively alleviate allergic responses. Tian et al. showed the potential of *B. animalis* KV9 to alleviate β-globulin induced food allergy in BALB/c mice (Tian et al., 2022). Moreover, we have previously shown that neonatal colonization of germ-free mice with *B. longum* ssp. *longum* CCM 7952 prevented sensitization to major birch pollen allergen Bet v1 (Schwarzer et al., 2013). Of note, intranasal administration of the same bifidobacterial strain exhibited allergy-reducing properties in ovalbumin (OVA)-sensitized mice (Pyclik et al., 2021).

We showed the ability of live as well as heat-killed *Bifidobacterium adolescentis* CCDM 368 (Bad368) to modulate the OVA-stimulated cytokine release from cells isolated from OVA-sensitized mice. Given the functionality of the heat-treated Bad368, we attempted to decipher which of the cell wall-associated postbiotics can actively participate in the Bad368 modulatory properties. Here, we demonstrate that one of the PSs, Bad368.1 with a unique structure, actively participates in the Bad368 immunomodulatory activities and is efficiently engulfed by lung epithelial cells and transferred to dendritic cells. Finally, the comprehensive chemical and NMR spectroscopy analysis allowed us to determine the structure of Bad368.1 PS, which we consider a prerequisite for potential use as a postbiotic in further medical applications.

2. Materials and methods

2.1. Bifidobacterium adolescentis CCDM 368 cultivation

Bifidobacterium adolescentis CCDM 368 (Bad368) from human adult feces was obtained from the Czech Collection of Diary Microorganisms (CCDM, Laktoflora, Milcom, Tábor, Czech Republic). The isolates were cultivated for 72 h in MRS broth (Sigma Aldrich) with 0.05 % L-cysteine (Merck Millipore) at 37 °C in an anaerobic chamber (Oxoid, 80 % N$_2$, 10 % CO$_2$, 10 % H$_2$). Before the start of the experiments, Bad368 was centrifuged (4500 ×g, 15 min, 4 °C) and washed with sterile phosphate-buffered saline (PBS). Finally, the bacterial pellet was frozen, freeze-dried and used for further isolations.

2.2. Isolation and purification of antigens

2.2.1. Polysaccharides

The isolation protocol was conducted according to Górska et al. (Górska et al., 2010). Briefly, bacterial mass was sonicated, incubated with shaking in 10 % trichloroacetic acid (2.5 h; room temperature (23 °C), and centrifuged (15,000 ×g; 4 °C; 20 min). The supernatant was treated with 5 volumes of ethanol and incubated overnight at −20 °C. On the next day, the suspension was centrifuged (as before) and the obtained pellet was dialyzed to miliQ water for 24 h at 4 °C (MWCO 6–8 kDa, Roth) and freeze-dried. Later, NGS Chromatography System (Bio-Rad) equipped with a UV detector was used to separate the resulting PSs mixture with the use of ion exchange chromatography (DEAE-Sephadex A-25 column; 1.6 × 20 cm (Pharmacia); buffer A: 20 mM Tris-HCl, buffer B: 2 M NaCl; linear-gradient (0 % B – 100 % B); 23 °C) and size exclusion chromatography (TSK HQ-55S column; 1.6 × 100 cm (Amersham Pharmacia Biotech); eluted with 0.1 M ammonium acetate; 23 °C). The phenol-sulfuric acid method was used to measure carbohydrate content in fractions collected after column separations (DuBois et al., 1956). Finally, obtained polysaccharide samples were analyzed using classical chemical methods and NMR spectroscopy (Górska et al., 2014).

2.2.2. Lipoteichoic acids

The LTA isolation procedure was conducted according to the modified protocol of Morath et al. (Morath et al., 2001). Briefly, bacterial mass was incubated with shaking in miliQ water and n-butanol mixture (1:1 v/v; 30 min; 23 °C). Next, the suspension was centrifuged (13,000 ×g; 20 min; 4 °C) and the pellet was re-extracted in the same manner (3 to 4 times). Finally, the water phase was collected, frozen, and freeze-dried. To purify and separate the obtained structures, crude LTA underwent ion exchange chromatography (DEAE-Sephadex A-25 column; 1.6 × 20 cm (Pharmacia); buffer A: 0.1 M sodium acetate (pH = 4.7), buffer B: 2 M NaCl; linear-gradient (0 % B – 100 % B); 23 °C) and hydrophobic interaction chromatography (Octyl Sepharose CL-4B; 1.6 × 60 cm (GE Healthcare); buffer A: 15 % n-propanol in 0.1 M sodium acetate (pH = 4.7), buffer B: 60 % n-propanol in 0.1 M sodium acetate (pH = 4.7); linear-gradient (0 % B – 100 % B); 23 °C) on the NGS Chromatography System equipped with UV detector. Finally, LTA fractions were determined with the use of the phenol-sulfuric acid method and underwent NMR spectroscopy analysis.

2.2.3. Peptidoglycan

The PG isolation was conducted according to the modified method of Schaub and Dillard (Schaub & Dillard, 2017). Briefly, bacterial mass was suspended in 25 mM phosphate buffer (100 ml, pH = 6) and added drop by drop to a boiling 8 % sodium dodecyl sulfate (100 ml, SDS). Then, the suspension was boiled (30 min; 100 °C), cooled, and ultra-centrifuged (200,000 ×g; 15 °C; 30 min). The obtained pellet was re-extracted, washed (4 to 6 times) with phosphate buffer, and freeze-dried. To receive a pure PG, 5 mg of the freeze-dried mass was dissolved in 2 ml of 50 mM Tris-HCl with 10 mM MgCl$_2$ (pH = 7.5) and underwent digestions, first for 6 h at 37 °C with 0.21 mg/ml of DNase and RNase, and next overnight with protease (0.45 mg/ml, 37 °C).

2.3. HEK-Blue™ cells cultivation and stimulation

Transfected human embryonal kidney (HEK) 293 cells were purchased from Invivogen and cultivated according to the manufacturer's instructions. Briefly, cells were cultured (37 °C, 5 % CO$_2$) in DMEM with 10 % (v/v) fetal bovine serum, 100 U/ml penicillin, 100 mg/ml

streptomycin, and 100 mg/ml Normocin™ (Invivogen) and selective antibiotics: (1) null: 100 μg/ml of Zeocin™ (Invivogen); (2) TLR2 and TLR4: 1 × HEK-Blue™ selection (Invivogen); (3) NOD2: 30 μg/ml of blasticidin (Invivogen) and 100 μg/ml of Zeocin™. After reaching 80 % of confluency, sterile PBS was used to collect the cells.

To determine the recognition pathways of studied antigens, 190 μl of the cells suspension (140,000 cells/ml in HEK-Blue™ Detection (Invivogen)) was added to each well in the 96-well plate. Next 10 μl of analyzed samples (1 μg/ml – 10 μg/ml) was added. Corresponding positive controls were used for tested cell lines: Pam3CSK4 (Pam3-CysSerLys4, Invivogen) for TLR2, LPS ultra-pure (lipopolysaccharide, Invivogen) for TLR4 and MDP (muramyl dipeptide, Invivogen) for NOD2 cells. The results were observed as a colorimetric reaction that was developing over time and the level of receptor activation was measured by absorbance read at $\lambda = 630$ and 650 nm. The results were presented as Δ absorbance at $\lambda = 630$ nm between tested samples and negative control (PBS-stimulated cells).

2.4. Stimulation of the splenocytes and dendritic cells isolated from the OVA-sensitized mice

2.4.1. Stimulation of the splenocytes isolated from OVA-sensitized mice

The immunomodulatory potential of Bad368 antigens was investigated *ex vivo* on the splenocytes isolated from OVA-sensitized BALB/c mice according to the method described by Pyclik et al. (Pyclik et al., 2021). Briefly, female mice (8–12 weeks of age) were sensitized by two intraperitoneal injections of 10 μg of OVA (Sigma Aldrich, grade V) mixed with 0.65 mg/100 μl of Alum (Serva) and one boosting injection of 15 μg of OVA mixed with 0.65 mg/100 μl of Alum (Serva) one week later. Seven days after the third sensitization, mice were anesthetized with 3 % isoflurane and euthanized by cervical dislocation. The animal experiment was approved by the committee for the protection and use of experimental animals of the Institute of Microbiology, The Czech Academy of Sciences (no. 91/2019). All procedures were performed in accordance with the EU Directive 2010/63/EU for animal experiments.

Spleens were aseptically removed and cells were isolated and cultured in RPMI 1640 medium (Sigma Aldrich) supplemented with 10 % FBS (Fetal Bovine Serum, Gibco), 100 U/ml of penicillin, 100 μg/ml streptomycin, and 10 mM HEPES (Sigma Aldrich). Cells were counted and seeded on a 96-well plate (5 × 10^6 cells/ml, 100 μl/well), re-stimulated with OVA (100 μg/well, Purified OAC, Worthington), and treated with studied antigens (PSs 30 μg/ml, PG and LTA 10 μg/ml in PBS) for 72 h (37 °C, 5 % CO₂). The concentration of cytokines was measured in supernatants by the Milliplex Map Mouse Cytokine/Chemokine Panel (IL-4, IL-5, IL-13, IL-10, and IFN-γ) according to the manufacturer's instructions and analyzed with Luminex 2000 System (Bio-Rad Laboratories). Changes in the levels of the Th1/Th2 cytokines were analyzed and presented as a percentage ratio between tested samples and the OVA-positive control (OVA re-stimulated splenocytes only) referred to as 100 %. Unstimulated cells were used as a negative control (medium without OVA).

2.4.2. Isolation and stimulation of the bone marrow-derived dendritic cells

Bone marrow-derived dendritic cells (BM-DCs) were isolated according to the previously described method (Górska et al., 2014). All procedures were performed in accordance with the EU Directive 2010/63/EU for animal experiments. Briefly, cells were rinsed from femurs and tibias of female BALB/c mice, placed in RPMI 1640 medium, centrifuged (215 ×g, 5 min), and counted. Next, the cells were put on a Petri dish in a medium supplemented with 10 % FBS, 150 μg/ml gentamycin (Sigma Aldrich), and 20 ng/ml murine granulocyte-macrophage colony-stimulating factor (GM-CSF, Invitrogen), and incubated for 7 days with the addition of the fresh medium on the 3rd and 6th day (37 °C, 5 % CO₂). BM-DCs were detached, counted, and seeded on the 48-well plate (1 × 10^6 cells/well) and stimulated with studied antigens (PSs 30 μg/ml, PG and LTA 10 μg/ml in PBS) for 20 h (37 °C, 5

% CO₂). Finally, the levels of IL-10, IL-6, IL-12p70, and TNF-α in culture supernatants were determined by ELISA Ready-Set-Go! kits (eBioscience) according to the manufacturer's instructions.

2.5. Antigen uptake and transfer between mouse epithelial cells (TC-1) and dendritic cells (JAWS II)

2.5.1. Antigens staining

The staining protocol for PS, LTA, and PG was adapted from FluoroProbes reagent manuals with some changes. PS, LTA, or PG (1 mg) were suspended in 400 μl 0.1 M sodium acetate (pH = 5.5) and metaperiodate (20 mM) and incubated at 4 °C for 30 min. Then, the solution was mixed with 100 μl 40 mM 1-Pyrenebutyric hydrazide (PBA) (Sigma Aldrich) in DMSO. The mixture was incubated for 3 h (23 °C, in darkness, with agitation) and dialyzed to dH₂O water (4 °C, 18 h) using a dialysis cassette (Slide-A-Lyzer Dialysis Cassette, Thermo Scientific). The PS and LTA content in the dialysate was assessed with DuBois assay (DuBois et al., 1956) by the absorbance measurement at $\lambda = 490$ nm. The PG content was checked by an absorbance read at $\lambda = 206$ nm and 254 nm. All the measurements were performed by Power Wave reader (BioTek) with the Gen5 Software (BioTek).

2.5.2. Antigen uptake by epithelial cell line (TC-1)

TC-1 cells (ATCC CRL-2785) were seeded on a 24-well plate (0.2 × 10^6 cells/ml) in a complete medium of DMEM + GlutaMax (Gibco), 10 % FBS (Gibco), and 1 % L-glutamine-Penicillin-Streptomycin solution and incubated for 2 h. Next, the stained antigens: 10 μg/ml of LTA, 10 μg/ml of PG, 30 μg/ml of PS were added to the cells and incubated for 4 h (37 °C, 5 % CO₂). To distinct the live population of TC-1 cells, the detached cells were stained with viability dye FV780 (BD Horizon, ref 565388) for 15 min at 23 °C. Next, the cells were washed and suspended in 1 % FBS/PBS before flow cytometry analysis (BD LSR Fortessa, BD Biosciences). The main population was marked based on the forward and side scatter. Debris was excluded by the FCS-H/FSC-A gating. The dead population was excluded from the analysis by the forward scatter vs viability dye. Obtained data were analyzed by FlowJo VX.07 software.

2.5.3. Antigen transfer between mouse epithelial (TC-1) and dendritic cells (JAWS II)

JAWS II cells (ATCC CRL-11904) were cultivated in Alpha MEM medium (Gibco) with 10 % FBS (Gibco), 1 % L-glutamine-Penicillin-Streptomycin solution, 1 mM sodium pyruvate (Sigma Aldrich), and 5 ng/ml GM-CSF in an incubator (37 °C, 5 % CO₂). Before co-culture, JAWS II were stained with red fluorescent dye PKH26 (Sigma Aldrich) according to the manufacturer's procedure, and 0.2 × 10^6 cells were seeded on a 24-well plate and incubated for 1.5 h. Simultaneously, TC-1 cells were grown and loaded with stained antigens as described in 2.5.2 and added to the stabilized JAWS II culture in an approximate ratio of 1:1 in a complete Alpha MEM medium. Cells were observed under the microscope (Axio Observer, Zeiss) for 24 h (37 °C, 5 % CO₂) or were co-cultured for the same amount of time for the flow cytometry analysis (as described in 5.2). In transfer studies, % of cells that acquired tested antigens was calculated exclusively for JAWS II (cells from quartiles Q1 and Q2, stained with PKH26 = 100 %).

2.6. Structure determination of the Bad368.1 polysaccharide compound

2.6.1. NMR spectroscopy and size determination

The NMR spectra were obtained on a Bruker 600 Hz Avance III spectrometer using a 5 mm QCI ¹H/¹³C/¹⁵N/³¹P probe equipped with a z-gradient. The data were acquired using the TopSpin 3.1pl6 software and processed with TopSpin 4.0.7 and SPARKY (Goddard 2001). PSs (10 μg) were dissolved in deuterium oxide and the one- (¹H, ³¹P) and two-dimensional NMR experiments (¹H-¹H-COSY, ¹H-¹H TOCSY, ¹H-¹H NOESY, ¹H-¹³C HSQC, ¹H-¹³C HMBC, ¹H-³¹P HSQC, and HSQC-TOSCY)

were carried out at 50 °C using pulses sequences from the Bruker library. The mixing times for TOCSY were 30, 60, and 100 ms, and for NOESY 100 and 300 ms. The delay time in HMBC was 60 ms. The chemical shifts for NMR signals were referenced by using acetone as an internal reference (δ_H 2.225 ppm, δ_C 31.05 ppm). To determine the absolute configuration of monosaccharides moieties present in all Bad368 PSs ^{13}C NMR chemical shifts were compared with the reference data (Shashkov et al., 1988).

The average molecular mass of each PS was determined by GPC (Dionex Ultimate 3000) on an OHpak SB-806 M HQ column (8 × 300 mm, maximum pore size 15,000 Å; Shodex) with dextran standards (MW 12, 25, 50, 80, 150 and 270 kDa). 0.1 M ammonium acetate buffer was used as the eluent. The flow rate was 0.5 ml/min and the run was monitored with a refractive index detector (RI 102; Shodex). The working detector temperature and sensitivity were adjusted to 35 °C and 512×, respectively. System control, data acquisition, and treatments were performed using the Chromeleon software (Dionex) (Górska et al., 2016).

2.6.2. Chemical analysis

Monosaccharide content of the purified PS was determined by sugar analysis as described previously (Sawardeker et al., 1965). Briefly, 0.3 mg of PS was hydrolyzed with 10 M HCl (80 °C, 25 min) and dried under a stream of N_2. Next, samples were reduced to sugar alditols using 10 mg/ml $NaBH_4$ (10 °C; overnight incubation). On the next day, the reduction was stopped by the addition of the 80 % acetic acid and free -OH groups were acetylated with methylimidazole and acetic anhydride. Next, the obtained alditol acetates were extracted 3 times by water: dichloromethane (1:1, v/v) mixture. Finally, the organic phase was collected, dried under a stream of N_2, and kept in the fridge before gas-liquid chromatography–mass spectrometry (GLC-MS) analysis. Samples obtained after sugar analysis were mixed with sugar standards to confirm monosaccharide composition in tested PSs.

To gain information about monosaccharide linkage and substitution positions, methylation analysis was performed. 2 mg of PS was dissolved in DMSO, treated with NaOH, and sonicated. To methylate free -OH groups, samples were incubated with iodomethane. Next, acetic acid was used to neutralize the pH of the samples and the methylated PS was extracted by a mixture of chloroform: water (1:1, v/v) (Ciucanu & Kerek, 1984). The obtained solution was dried under a stream of N_2 and subjected to sugar analysis as described previously, except that 10 mg/ml $NaBD_4$ was used for reduction instead of the $NaBH_4$. Dried samples were dissolved in ethyl acetate and analyzed by GLC-MS on the ITQ 700 Thermo Focus GC system equipped with Zebron ZB-5HT Inferno capillary column (Phenomenex) with a temperature gradient from 150 °C to 270 °C (8 °C/min). All data were obtained and analyzed by the Xcalibur™ software (Thermo Fisher).

2.7. Statistical analysis

All experiments were repeated in at least two technical and two biological repetitions. Data are presented as mean ± SD and differences were analyzed with one-way ANOVA together with Dunnett's multiple comparisons. All statistical analyses and visualizations were prepared with the use of Graph Pad Prism version 9.

3. Results

Both live and heat-inactivated *Bifidobacterium adolescentis* CCDM 368 bacteria show the ability to reduce the Th2-related cytokine production of IL-5, IL-4, and IL-13 in OVA-stimulated cells derived from OVA-sensitized mice (Supplementary Fig. S1). Thus, we decided to define the molecules responsible for the immunomodulatory effect present in inactivated bacterial cells. Bad368 antigens that include PSs, PG, and LTAs were isolated and purified. We found out that Bad368 produce three different PSs which will be referred to as the biological fraction 1,

2, and 3 (Bad368.1, Bad368.2, and Bad368.3, respectively) (Supplementary Fig. S2). On the contrary, the LTA and PG purification revealed the presence of only one fraction of each antigen.

3.1. Bifidobacterium adolescentis CCDM 368 antigens are recognized by innate immune receptors

HEK cells transfected with the innate immune receptors from the TLR and NOD receptor family were used to demonstrate the recognition pathways induced by isolated molecules. Studied antigens were added to the cells and colorimetric reaction was developed. We observed that LTA was recognized by TLR2, whereas PG led to the activation of TLR2 and NOD2. Polysaccharides Bad368.1 and Bad368.3 caused a robust activation of TLR2, they were also able to induce TLR4 response. Interestingly, Bad368.2 wasn't recognized by any of the tested immune receptors. Null cells that lack analyzed receptors were used as a negative control for transfected cell lines (Supplementary Fig. S3).

3.2. Bifidobacterium adolescentis CCDM 368 antigens differently affect the OVA-induced cytokine production by splenocytes

Splenocytes isolated from ovalbumin (OVA)-sensitized female BALB/c mice were used to evaluate the potential of isolated molecules to modulate the OVA-induced cytokine production. We observed different effects for each of the PS fractions: Bad368.1 PS significantly inhibited the production of IL-5 while Bad368.3 significantly decreased the level of both IL-4 and IL-5 when compared to OVA-stimulated cells. All three fractions showed tendency to decrease IL-13 (Fig. 1). Stimulation with PG and LTA did not show any notable changes in the levels of Th2-related cytokines. In the case of regulatory IL-10, PG, and Bad368.1 PS were able to induce high levels of this cytokine. Strikingly, it was Bad368.1 PS that caused a robust production of pro-inflammatory cytokines IFN-γ and IL-6 suggesting the Th1-inducing properties. We also observed the induction of IL-6 cytokine after PG and Bad368.3 stimulation as well as increased production of IFN-γ, however the level of the latter was significantly lower when compared to Bad368.1 PS.

3.3. Bad368.1 polysaccharide induces cytokine production in bone marrow-derived dendritic cells

From the tested Bad368 molecules we selected representative antigens: Bad.368.1 PS, PG, and LTA that exhibited interesting immunomodulatory properties for further studies. First, we decided to analyze cytokine production in BM-DCs treated with the selected antigens. Interestingly, we observed that their response depended on the antigen type. Bad368.1 PS showed a tendency to improve TNF-α and IL-10 levels and as the only one among other antigens caused a significant increase in IL-6 production. Upon exposure to PG, BM-DCs produced a very low level of IL-10, TNF-α, and IL-6, whereas stimulation with LTA slightly increased the level of IL-10 (Fig. 2). None of the tested molecules were able to induce IL-12p70 production in BM-DCs (data not shown).

3.4. The efficiency of Bad368.1 polysaccharide, lipoteichoic acid and peptidoglycan uptake by airway epithelial cells (TC-1) and antigen transfer to dendritic cells (JAWS II) vary depending on the molecule

To confirm the efficient recognition and engulfment of studied antigens, the uptake analysis was performed with labeled Bad368.1 PS, PG, and LTA by flow cytometry. The analysis indicated the engulfment of all antigens, with the highest mean value for Bad368.1 PS (99 %), then for PG (81 %). The lowest mean value was noted for LTA (8 %) (Fig. 3, Supplementary Fig. S4). The obtained results indicated the presence of two populations of epithelial cells: 1) which internalized the labeled antigen (positive population), and 2) which did not (negative population).

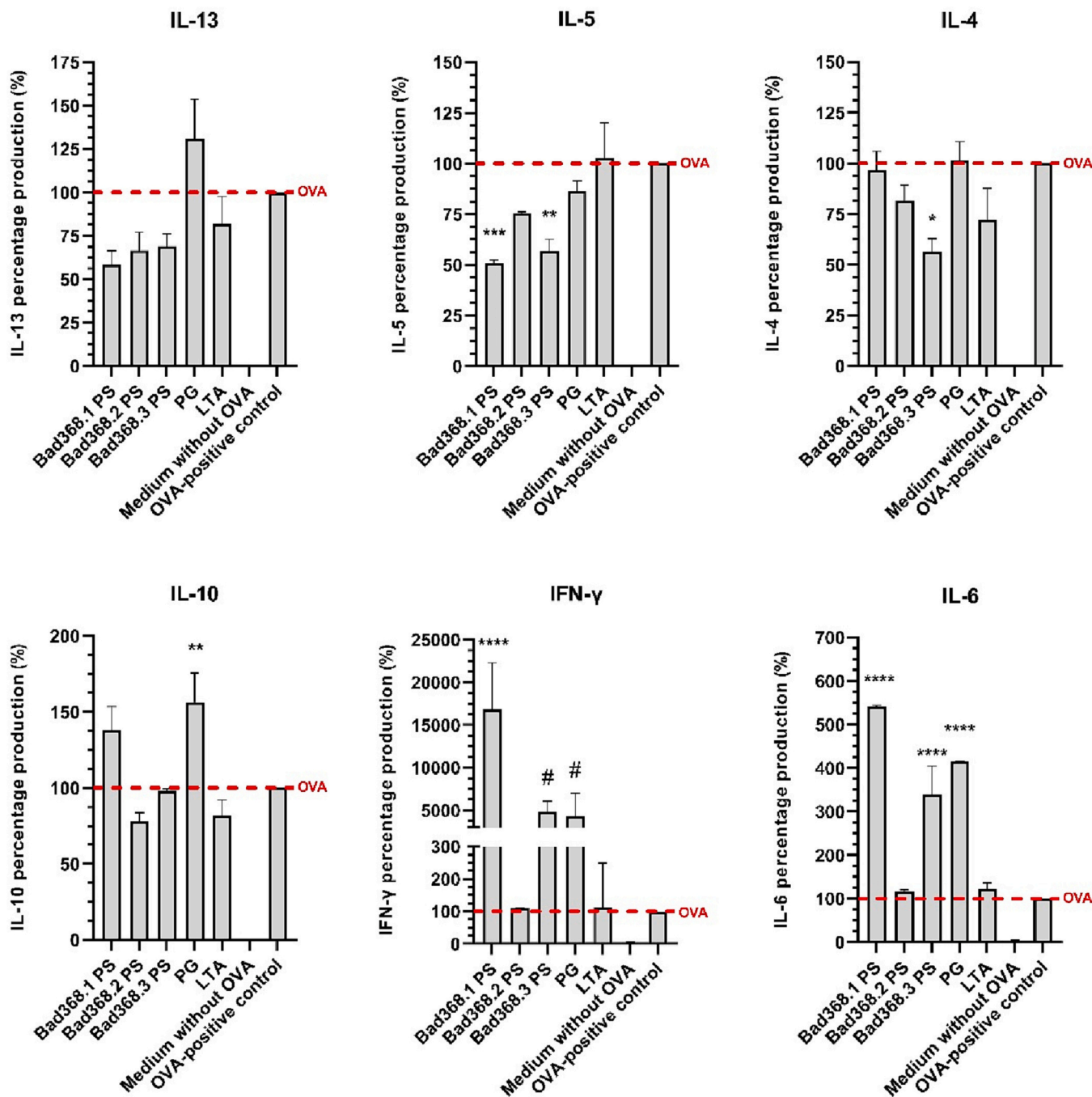Next, we examined the antigen transfer between epithelial cells and

Fig. 1. Cytokine production by OVA-sensitized splenocytes after stimulation with *Bifidobacterium adolescentis* CCDM 368 antigens. Mouse splenocytes were stimulated with OVA (500 μg/ml) together with antigens at a concentration of 10 μg/ml for PG and LTA and 30 μg/ml for PSs (Bad368.1, Bad368.2, Bad368.3) or PBS (OVA-positive control). Unstimulated splenocytes (medium without OVA) served as a negative control. Data are shown as mean ± SD of 2 mice and expressed as a percentage ratio between tested samples and the OVA-positive control. One-way ANOVA with Dunnett's multiple comparison tests were performed and significant differences compared to OVA-control (red dashed line) were calculated (**** $p \leq 0.0001$, *** $p \leq 0.001$, ** $p \leq 0.01$, * $p \leq 0.05$). Additionally, for IFN-γ significant differences between Bad368.1 PS and other PSs (Bad368.2 PS and Bad368.3 PS) were marked with # ($p \leq 0.0001$).

antigen presenting cells (APCs), in which antigen-treated TC-1 cells were incubated in co-culture with JAWS II cells for 18 h. The efficiency of this process was determined by fluorescence microscopy (Fig. 4A) and flow cytometry (Fig. 4B and C). As previously, the ability of the DCs to acquire antigens differed depending on the type of the antigen. In the case of Bad368.1 PS, the uptake by DCs was visible under a microscope. It was also confirmed by flow cytometry analysis, which indicated the presence of labeled Bad368.1 PS in 71.3 % of JAWS II cells (exclusively) (Fig. 4C). Acquisition of LTA by DCs was at the level of approx. 48.8 % as determined by the flow cytometry analysis and confirmed under a

microscope, whereas no PG uptake by JAWS II cells was detected.

3.5. Structural analysis of Bad368.1 polysaccharide

Bad368 produces a complex PS blend. The crude PS was subjected to purification by ion-exchange and size exclusion chromatography methods. Analysis of the ^{1}H NMR spectra allowed us to distinguish three structurally different PS fractions that were called Bad368.1 PS, Bad368.2 PS, and Bad368.3 PS (Supplementary Fig. S2).

Further, to investigate monosaccharide composition in each fraction,
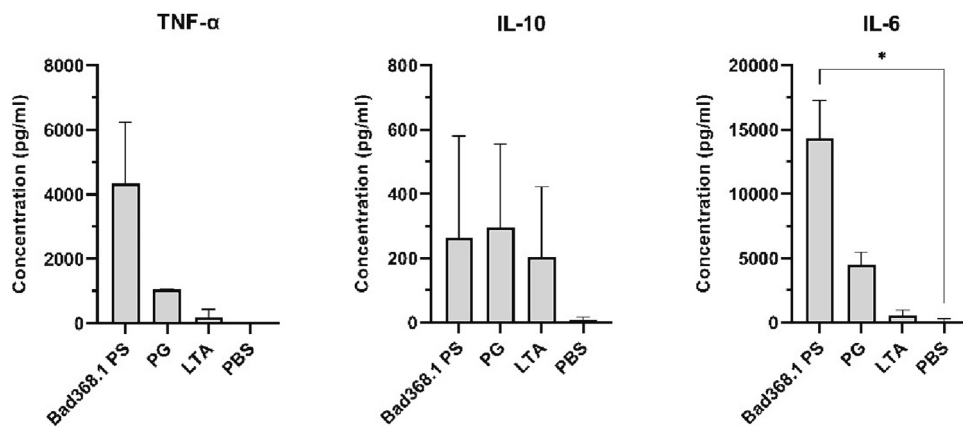
Fig. 2. Bone marrow-derived dendritic cells cytokine production after stimulation with *Bifidobacterium adolescentis* CCDM 368 antigens. Mouse BM-DCs were treated with PBS (negative control) or studied molecules at a concentration of 10 μg/ml for PG and LTA and 30 μg/ml for PSs. Data are shown as mean ± SD of 2 mice and one-way ANOVA and Dunnett's multiple comparison tests were performed and significant differences were calculated (* $p \leq 0.05$).
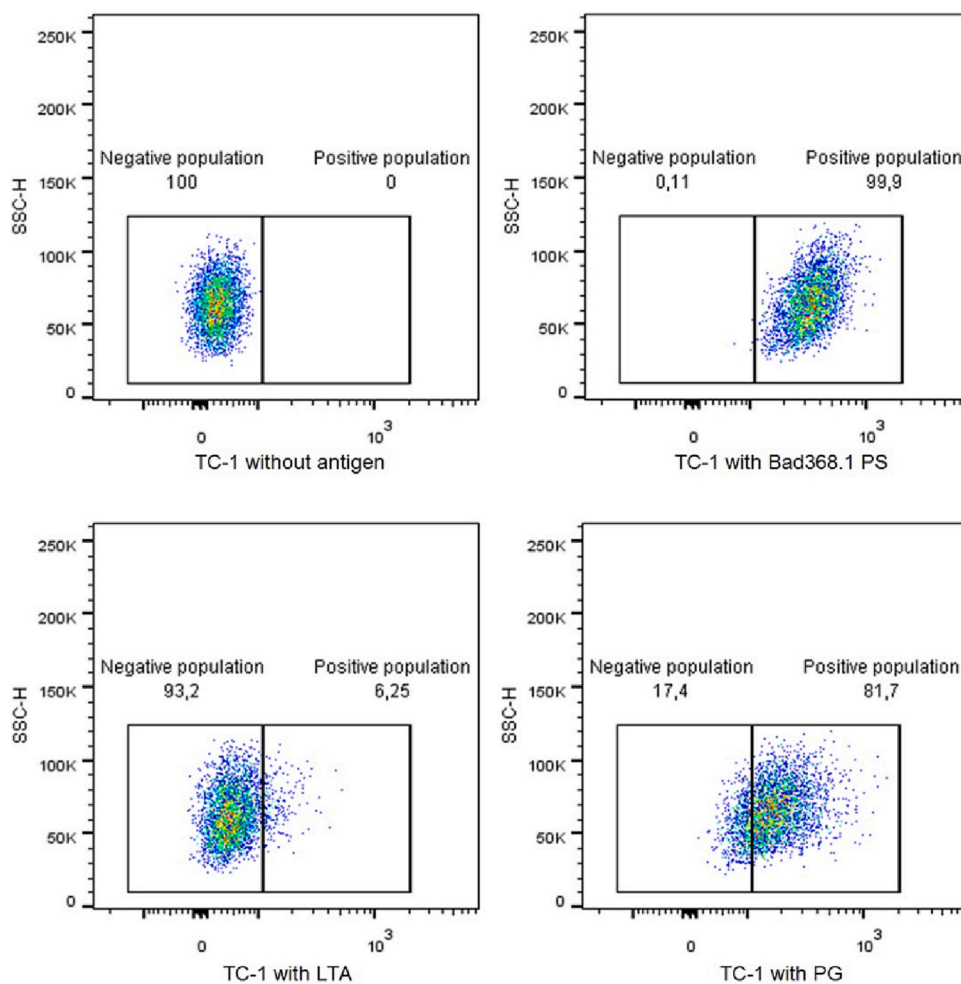
Fig. 3. A dot-plot analysis of the antigen uptake by epithelial cells (TC-1). The cells were stimulated by 30 μg/ml of PS, 10 μg/ml of LTA, and 10 μg/ml of PG for 4 h. The internalization of the antigen was determined as a difference between the population with (positive population) or without (negative population) detectable antigen (Bad368.1 PS, LTA or PG) (SSC-H – side scatter high). Representative dot plots were presented. The experiment was repeated in 2 biological repetitions.

sugar analysis was performed and molecular mass was determined. The GLC-MS sugar analysis revealed that:

a. **Bad368.1 PS** consists of L-Rha, D-Glc, and D-Gal in a molar ratio of 1:3:1.25. The average molecular mass is approximately 9.99×10^6 Da.

b. **Bad368.2 PS** consists of L-Rha, D-Glc, and D-Gal in a molar ratio of 1:1.4:3. The average molecular mass is approximately 1.24×10^4 Da.

Bad368.1 PS   **LTA**   **PG**
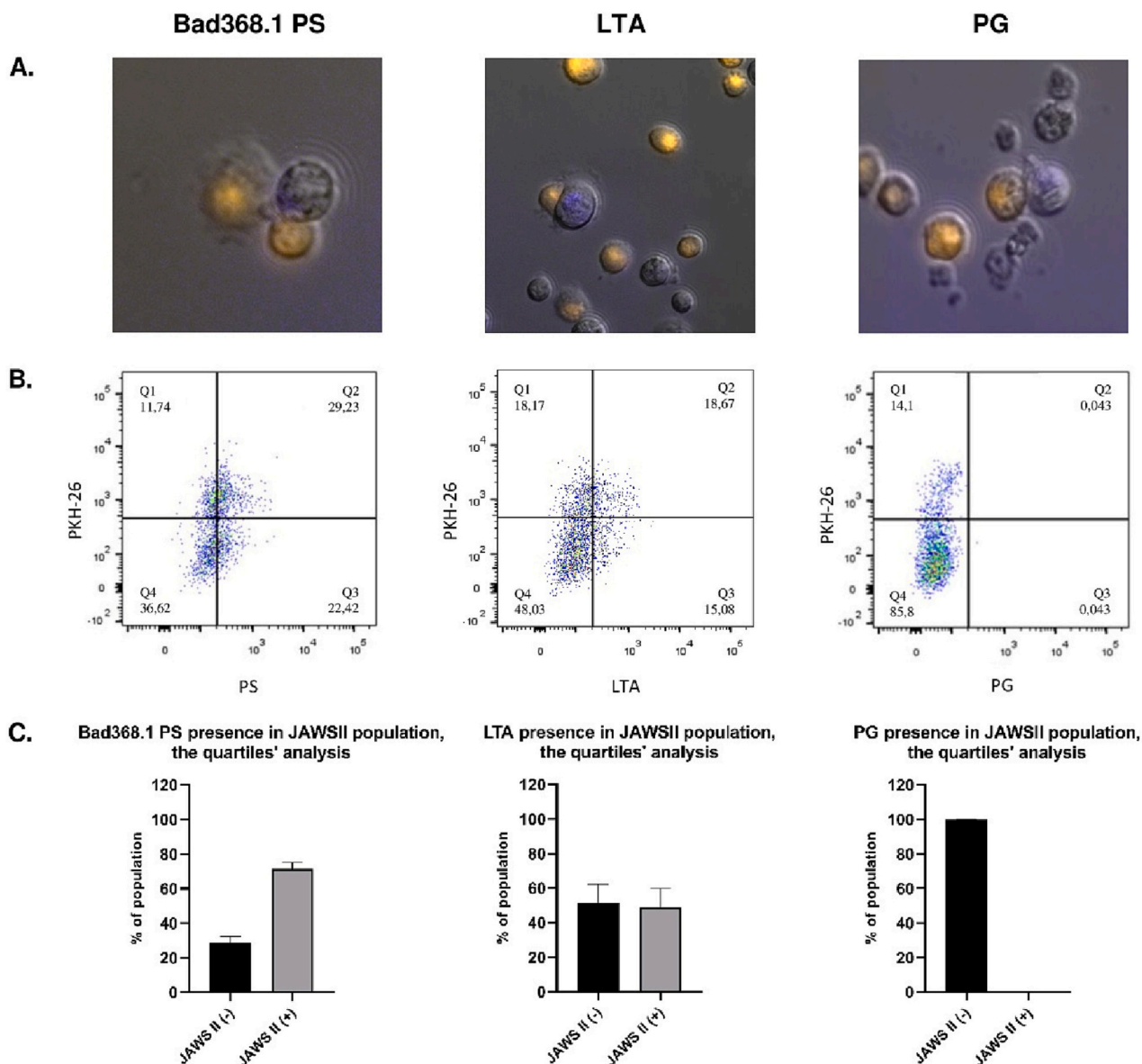
Fig. 4. Antigen transfer from epithelial cells to dendritic cells. A. Fluorescent microscopy results (yellow cells: JAWS II stained with PKH-26; violet cells: TC-1 with labeled antigen). B. Representative dot plots obtained by flow cytometry. C. Flow cytometry results assessed on comparison of the fluorescence signal between quartile Q1 (% of JAWS II cells without antigen - JAWS II (−)) and Q2 (% of JAWS II cells with tested antigen - JAWS II (+)). The experiment was repeated in 2 biological repetitions.

c. **Bad368.3 PS** consists of D-Glc and D-Gal in a molar ratio of 1:2.3. The average molecular mass is approximately 1.27×10^4 Da.

Immunomodulatory studies on splenocytes and BM-DCs revealed interesting immunomodulatory properties only in the case of Bad368.1 PS (Figs. 1 and 2), thus we decided to determine the structure of this PS. At first, methylation analysis was performed to characterize the linkages and substitution positions in this PS. It revealed the presence of 3-Rha*p*, 3-Gal*p*, 2-Glc*p*, and 4-Glc*p*.

The ^{1}H NMR spectrum displayed three different types of signals: the anomeric region (5.6–4.5 ppm), the ring protons region (4.5–3.2 ppm), and the methyl group region. Six distinct signals were present in the anomeric region and two signals in the methyl group region. The absence of ^{31}P signals in the ^{31}P NMR spectrum indicated that Bad368.1 was not phosphorylated.

The ^{1}H-^{13}C HSQC spectrum showed six cross peaks in the region of anomeric resonances corresponding to hexapyranosyl residues indicating that Bad368.1 is made of a hexasaccharide repeating unit (HSQC

spectrum with assigned signals is presented in Fig. 5). The chemical shifts of proton and carbon signals from the six sugar residues were assigned from a combination of 2D NMR experiments, COSY, TOCSY at several mixing times, HSQC, HSQC-TOCSY, NOESY, and HMBC (Tables 1 and 2) (Supplementary Figs. S5–S8). The sugar residues were marked with the uppercase letter starting from the most downfield signal in the ^{1}H NMR spectrum.

Analysis of the TOCSY and HSQC-TOCSY spectra showed that residues C, E, and F have *gluco*-configuration as shown by the scalar correlations from the anomeric signal to the other ring signals. Residue A was assigned to the *galacto*-configuration since scalar correlations were observed in the TOCSY and HSQC-TOCSY from the anomeric signal and the other ring signals until the H4/C4 resonance. The H5/C5 signals were assigned from the NOE connectivity from H3 to H5 and from the connectivity in the HMBC spectrum between H1 and C5. The H6/C6 signals were further identified from the scalar connectivities with H5/C5 in the TOCSY and HSQC-TOCSY spectra. Residues B and D were identified as rhamnose by the characteristic methyl resonance of the 6-deoxy
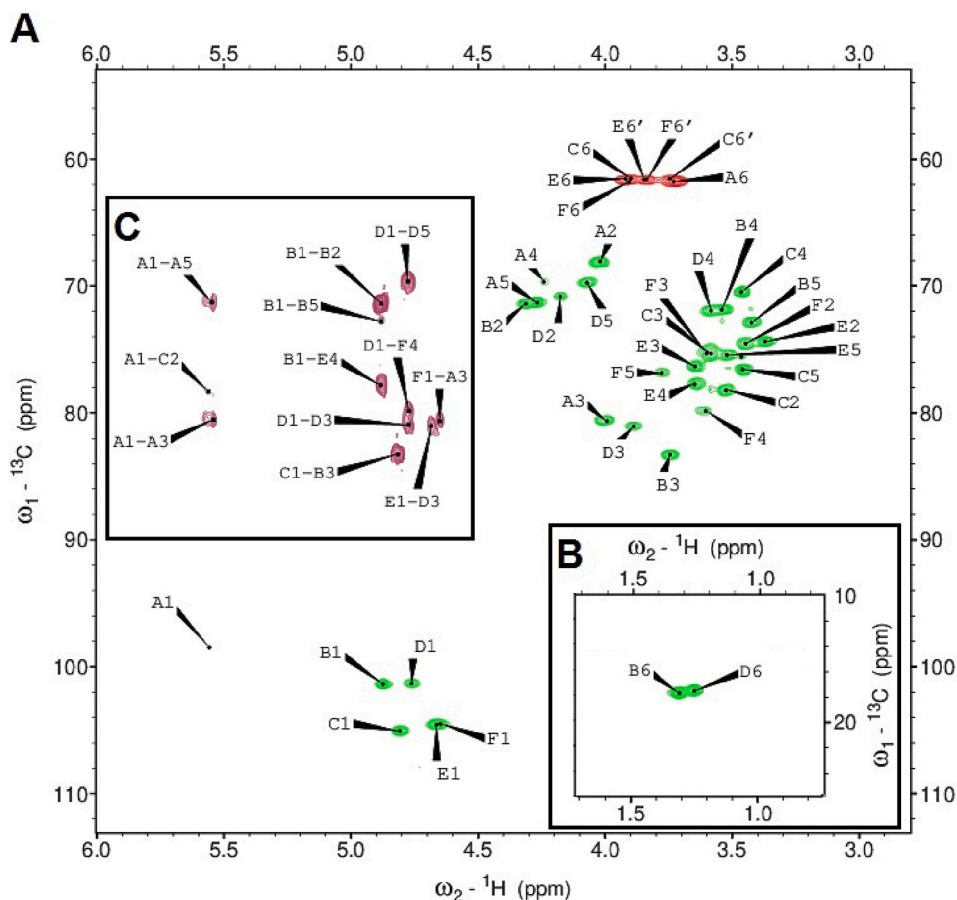
Fig. 5. A. ^{1}H-^{13}C HSQC NMR spectrum of Bad368.1 polysaccharide at 50 °C. The anomeric signals are located in the chemical shift range of 4.2–5.8 ppm and the ring signals between 3.2 and 4.5 ppm. **B.** The H-6/C-6 signals for rhamnoses (residue B and D). **C.** The part of the HMBC spectrum which corresponds to the anomeric signals in HSQC spectra.

Table 1
^{1}H and ^{13}C NMR chemical shifts of resonances of Bad368.1 polysaccharide from *Bifidobacterium adolescentis* CCDM 368.

Sugar residue		^{1}H, ^{13}C chemical shifts (ppm)					
		H-1, C-1	H-2, C-2	H-3, C-3	H-4, C-4	H-5, C-5	H-6; H-6', C-6
A	→3)- α-D-Gal*p*-(1→	5.56	4.03	4.01	4.25	4.28	3.74
		98.4	68.1	80.5	69.6	71.2	61.7
B	→3)-β-L-Rha*p*-(1→	4.88	4.32	3.75	3.55	3.43	1.33
		101.2	71.3	83.2	71.8	72.8	17.6
C	→2)-β-D-Glc*p*-(1→	4.82	3.54	3.59	3.47	3.47	3.91; 3.75
		104.9	78.2	75.3	70.4	76.4	61.5
D	→3)-α-L-Rha*p*-(1→	4.78	4.18	3.90	3.59	4.08	1.27
		101.2	70.8	80.9	71.9	69.6	17.4
E	→4)-β-D-Glc*p*-(1→	4.68	3.38	3.65	3.65	3.53	3.93; 3.84
		104.4	74.3	76.3	77.7	75.4	61.6
F	→4)-β-D-Glc*p*-(1→	4.66	3.46	3.59	3.63	3.75	3.93; 3.84
		104.4	74.5	75.3	79.8	77.0	61.6[a]

[a] Could not be assigned unambiguously.

sugar at 1.33 and 1.27 ppm in combination with the observation of only one cross-peak in the TOCSY spectrum from H1 to H2. All spin systems were assigned in the TOCSY and HSQC-TOCSY using the methyl groups as a starting point.

The anomeric configuration of C, E, and F was identified as β due to the $^3J_{H1H2}$-values >7 Hz. Residue A has the α-configuration as shown by the small $^3J_{H1H2}$-value of 3.0 Hz. For the B and D rhamnose residues, the distinction between α- and β- form is not straightforward since the couplings are <3 Hz and not resolved in the spectra due to line broadening. It has been shown that the position of the signal at C5 can be used

Table 2
Selected inter-residue correlations from ^{1}H,^{1}H NOESY and ^{1}H,^{13}C HMBC spectra of Bad368.1 polysaccharide.

	Residue	H-1/C-1	Connectivity to		Inter-residue
		δ_H/δ_C	δ_C	δ_H	Atom/residue
A	→3)-α-D-Gal*cp*(1→	5.56/98.4	78.2	3.54	C-2, H-2 of **C**
B	→3)-β-L-Rha*p*-(1→	4.88/101.2	77.7	3.65	C-4, H-4 of **E**
C	→2)-β-D-Glc*p*-(1→	4.82/104.9	83.2	3.75	C-3, H-3 of **B**
D	→3)-α-L-Rha*p*-(1→	4.78/101.2	79.8	3.63	C-4, H-4 of **F**
E	→4)-β-D-Glc*p*-(1→	4.68/104.4	80.9	3.90	C-3, H-3 of **D**
F	→4)-β-D-Glc*p*-(1→	4.66/104.4	80.5	4.01	C-3, H-3 of **A**

to distinguish between an α- or a β-linked rhamnose with a C5 at δ 70.5 ppm indicating an α-linked Rha while a C5 with δ at 73.2 ppm indicates a β-Rha$p$ (Carillo et al., 2009; Lipkind et al., 1988; Mattos et al., 2001; Senchenkova et al., 1999; Vinogradov et al., 2003). Thus, residue B with C5 at 72.9 ppm can be assigned as β-Rha while residue D with C5 at 69.7 ppm can be assigned as a α-Rha. The α-Rha configuration of residue D was also confirmed by the absence of intraglycosidic NOEs between H1 and H3, H5 while the β-configuration of residue B was confirmed by NOEs from H1 to H3 and H5 (Vinogradov et al., 2003).

The glycosidic bond connections/linkages between the constituent monosaccharides were obtained from the ^{1}H-^{1}H NOESY and ^{1}H-^{13}C HMBC spectra (see Table 2). The glycosylation pattern was confirmed by the downfield shift of the signals of C3 Gal$p$ (**A**), C3 Rha$p$ (**B** and **D**), C2 Glc$p$, and (**C**) C4 Glc$p$ (**E** and **F**) if compared to the non-substituted sugars. To determine the absolute configuration of the Bad368.1 PS monosaccharide moieties ^{13}C NMR chemical shifts were compared with the reference data (Shashkov et al., 1988). The following sequence was thus determined: →2)-β-D-Glc$p$-(1 → 3)-β-L-Rha$p$-(1 → 4)-β-D-Glc$p$-(1 → 3)-α-L-Rha$p$-(1 → 4)-β-D-Glc$p$-(1 → 3)-α-D-Gal$p$-(1→, or with upper-case letters: **C-B-E-D-F-A**. The proposed structure of the repeating unit is presented in Fig. 6.

4. Discussion

The present study was initiated to investigate the immunomodulatory properties of antigens isolated from different *Bifidobacterium* strains that included *B. adolescentis* CCDM 368 and to test their potential as active postbiotics. The idea to investigate the surface molecules of this particular strain was based on *in vitro* experiments performed with untreated and heat-treated bacteria. Obtained results showed that even after heat-inactivation, Bad368 still reduced OVA-induced Th2-related production of IL-5, IL-4, and IL-13 cytokines in splenocytes from OVA-sensitized mice. Since the immunomodulatory properties of the strain were retained in heat-killed bacteria, we aimed at identifying bacteria surface antigens that might be responsible for the observed effect. Thus, we isolated, purified, and evaluated the role of the Bad368 LTAs, PG, and PSs. Interestingly, Bad368.1 PS significantly increased the level of IFN-γ and IL-10 while simultaneously reducing the production of IL-13 and IL-5 in splenocytes isolated from OVA-sensitized mice. In the context of potential anti-allergic properties, a high level of IFN-γ is desirable, because this cytokine can further act as a suppressor for Th2 and switch the response towards Th1 cells (Amrouche et al., 2006; Ivashkiv, 2018). On the contrary, the role of IL-10 is ambiguous. Higher secretion of this cytokine might be related to its production by (1) Treg cells, which leads to the diminished Th2 responses, or (2) Th2 cells and IL-10 function as a guard cytokine that keeps the IFN-γ levels within safe ranges (Robinson et al., 2004). Polymer Bad368.3 exhibited similar properties to Bad368.1 PS but in a weaker manner while Bad368.2 was able to induce neither IFN-γ nor IL-6.

The functions of polysaccharides are mainly affected by their sugar composition and the connections they made within a chain unit. Thus, the chemical structure of Bad368 PSs may impact their biological properties. Our observations are in line with previous studies showing that the ability of PSs from various bifidobacteria to affect immune cell functions depends on their structure. Verma et al. investigated *B. bifidum* and its role in the generation of Foxp3+ cells. Among different PS fractions, only CSGG (consisting of at least 4 different PSs in a form of

neutral β-glucans/galactans) was able to activate DCs via TLR2 receptor which resulted in higher levels of TGF-β and IL-10 (Verma et al., 2018). Administration of the PS from *B. longum* subsp. *longum* 35624™ reduced the number of inflammatory cells in peribronchial and perivascular lung tissue in mice with OVA-induced allergic inflammation. Within lung lavages, the eosinophil levels were decreased while the IL-10 level was increased. Moreover, lung tissue studies revealed inhibited expression of Th2-related IL-4 and IL-13 (Schiavi et al., 2018). Our results of BM-DCs and splenocytes stimulation outlined that Bad368.1 PS and PG might be at forefront of interest since they were able to induce the Th1-related response.

Glucose and galactose are the main components of each of the Bad368 PSs. Moreover, rhamnose also occurs in Bad368.1 PS and Bad368.2 PS structures. Polymer Bad368.1 PS with a high average molecular mass of 9.99×10^6 Da is a linear heteropolysaccharide with a repeating unit consisting of six monosaccharide residues. The remaining Bad368.2 and Bad368.3 are characterized by the low average molecular mass of 1.24×10^4 Da and 1.27×10^4 Da, respectively. Both Bad368.1 PS and Bad368.3 PS were strong activators of the TLR2, they were also able to activate TLR4 receptors (Supplementary Fig. S3). Interestingly, Bad368.2 was able to induce only a weak TLR2 response, and no TLR4 or NOD2 response, which indicates that it may be recognized in a different manner. Laws et al. suggested that there is a link between sugar conformation and backbone linkages, and the chemical properties and function of PSs. He indicated that (1−>4) linkages and β-isomers are adding more stiffness to the PSs whereas (1−>3), (1−>2) linkages and α-isomers are more flexible and in general have stronger anti-microbial and anti-oxidant properties (Laws et al., 2001; Zhou et al., 2019). Bad368.1 PS is more abundant in (1−>2) and (1−>3) linkages and β-isomers that might influence its ability to modulate the immune response. Furthermore, some publications connect the role of bacterial PS with its size. Górska et al. showed that high molecular mass PS L900/2 exhibits regulatory properties meanwhile small molecular mass L900/3 induces a pro-inflammatory response in a mouse model of OVA-sensitization (Górska et al., 2017). However, it is inconsistent with our results since high molecular mass Bad368.1 PS was able to elicit both regulatory IL-10 and pro-inflammatory IFN-γ. Another factor that can have a great impact on PS properties is its charge. Studies performed by Speciale et al. on PS isolated from *B. bifidum* PRI1 showed differences in properties between neutral mix (CSGG) fraction that enhanced regulatory functions of the DCs and negatively charged (PBβG) PS that induced proinflammatory cytokine production (IFN-γ) (Speciale et al., 2019). Verma et al. reported that the neutral fraction of *B. bifidum* PS induced the generation of Foxp3+ regulatory T cells in mice when at the same time the negatively charged PS preparations did not exhibit the same properties (Verma et al., 2018). The chemical and NMR analysis did not show any modifications in the Bad368.1 PS chain like phosphorylation that would influence the charge of the PS. It was indicated that the charge of molecules can affect their processing by epithelial or immune cells depending on their polarity. Since the eukaryotic cell membrane is negatively charged, PSs with a positive/neutral charge can be easier internalized than the negatively charged one (Salatin & Yari Khosroushahi, 2017). Along these lines, we observed efficient engulfment of the polymer Bad368.1 PS by epithelial cells and its further transfer to DCs. Generally, PSs are characterized by a high affinity for the mucosal surface, therefore are widespread through the respiratory and gastrointestinal tract (Salatin & Yari Khosroushahi, 2017).
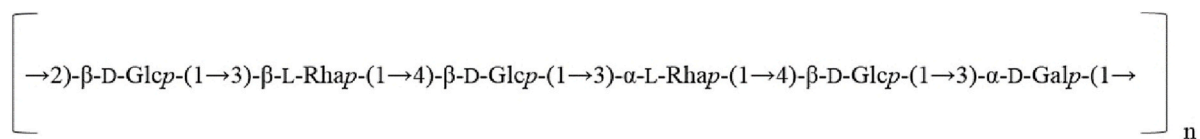
$$\left[\rightarrow 2)\text{-}\beta\text{-D-Glc}p\text{-}(1 \rightarrow 3)\text{-}\beta\text{-L-Rha}p\text{-}(1 \rightarrow 4)\text{-}\beta\text{-D-Glc}p\text{-}(1 \rightarrow 3)\text{-}\alpha\text{-L-Rha}p\text{-}(1 \rightarrow 4)\text{-}\beta\text{-D-Glc}p\text{-}(1 \rightarrow 3)\text{-}\alpha\text{-D-Gal}p\text{-}(1 \rightarrow \right]_n$$

Fig. 6. Structure of the hexasaccharide repeating unit of the Bad368.1 polysaccharide. The approximate number of units in the Bad368.1 polysaccharide equals n = 10,000.

A thorough literature review confirmed that the Bad368.1 PS was not described in different *Bifidobacterium* strains so far. Hosono et al. described water-soluble polysaccharide fraction from *B. adolescentis* M101-4 that in comparison to Bad368.1 PS has furanoses in its structure and no rhamnose residues (Hosono et al., 1977). Another example is a polysaccharide-glycopeptide complex isolated from *B. adolescentis* YIT4011 that contains dTal in the main chain (Nagaoka et al., 1988). Moreover, CSDB (Carbohydrate Structure Database) platform did not indicate the Bad368.1 PS in different organisms. Although, the presence of this structure in different bifidobacteria cannot be excluded. It must be underlined that the effect of the bacteria is the resultant of all of their antigens. The ratio in which the effector molecules are present on the bacteria surface is also important. In our previous studies on the function of *L. rhamnosus* LOCK 0900 polysaccharides we showed that the whole bacteria induced production of IL-10 in BM-DCs, whereas thier PSs did not stimulate the production of IL-10 or IL-12. Surprisingly, PSs due to their chemical features were able to modulate the immune responses to third-party antigens. Exposure to L900/2 enhanced IL-10 production induced by *L. plantarum* WCFS1, while in contrast, L900/3 enhanced the production of IL-12p70 in BM-DCs (Górska et al., 2014).

Results obtained after stimulation of splenocytes and BM-DCs, together with the outcome of the transfer studies, clearly indicate that Bad368.1 PS has the strongest potential among Bad368 antigens to modulate allergic diseases in humans. Due to the potential of newly described structure we decided to name it BAP1 for the further studies.

While discussing PG immunomodulatory properties, it is important to point out that Bad368 PG was able to induce both NOD2 and TLR2 receptors sensing. This is in agreement with Corridoni et al. data indicating that the antigen cross-priming and CD8+ T cells activation are associated with the upregulation of both receptors (Corridoni et al., 2019). We observed that Bad368 PG was able to stimulate the splenocytes to produce a considerable amount of IFN-γ and IL-10 and a significant amount of IL-6. However, the Bad368 PG did not reduce the level of Th2-related cytokines in OVA-sensitized and stimulated splenocytes culture. On the other side, PG improved the production of IL-10, TNF-α, and IL-6 in BM-DCs. Moreover, we have shown, that up to 75 % of TC-1 cells reacted to the PG's presence and internalized the antigen. Also, the PG uptake by the DCs was visible under a microscope up to 12–13 h. It is important to note that we used enzymatically purified PG fraction to minimalize the effect of the antigens present on its surface. Only a few publications describe the role of purified or partially purified PGs. In one of them, Li et al. focused on the role of the PG from *Lactobacillus acidophilus* KLDS 1.0738 on mice sensitized with β-lactoglobulin. Stimulation of murine macrophages with PG revealed its role in the induction of IFN-γ, IL-10, and TGF-β via the TLR2 pathway (Li et al., 2017). Another study performed on lactic acid bacteria extracts showed that selected bacteria strains were able to induce a significant amount of TNF-α and IL-6 in RAW 264.7 cells (Tejada-Simon & Pestka, 1999).

The LTA from the Bad368 strain did not reveal any potential to alleviate OVA-induced Th2-related cytokines in splenocytes nor induced significant cytokine response in BM-DCs. However, this does not exclude its role in the treatment of other diseases. Research focusing on LTA underlines the role of the TLR2 receptors in the recognition of this molecule which is in line with our results (Dessing et al., 2008; Schröder et al., 2003; Zeuthen et al., 2008). There is little information about the bifidobacterial LTAs' impact on the host. Studies of this compound derived from other probiotic bacteria such as lactobacilli confirm its crucial role in physiological and immunomodulatory functions. *Lactobacillus plantarum* L-137 studies indicated the LTA role in phagocytosis and induction of the splenic cells to produce IL-12p40 cytokine which is crucial in the Th1 responses (Hatano et al., 2015). Furthermore, Jeong et al. examined how the LTA structure affects the Th1-related TNF-α and regulatory IL-10 production in RAW 264.7 cells (Jeong et al., 2015). We indicated that LTA derived from *B. adolescentis* CCDM 368 is internalized by epithelial cells at a low level. However, in our model, almost half of the population of dendritic cells (JAWS II) intercepted the antigen from the epithelial cells, which indicates the antigen potential.

5. Conclusions

For the first time we comprehensively compared the biological activity of various *Bifidobacterium* surface antigens. We identified polysaccharide Bad368.1 which was able to efficiently induce the Th1-related response while decreasing the production of Th2 cytokines in allergen-stimulated splenocytes from OVA-sensitized mice. It also induced the Th1 cytokine production after stimulation of naïve BM-DCs. Moreover, this polysaccharide was well recognized by epithelial cells and transferred to DCs. The detailed investigation of its structure pointed out features that may contribute to the biological role of the Bad368.1 PS: lack of electric charge, high mass, monosaccharide content, and linkages. We foresee that this postbiotic molecule may be used in the future in the context of the prevention/treatment of allergy diseases.

CRediT authorship contribution statement

Katarzyna Pacyga-Prus: Methodology, Formal analysis, Investigation, Resources, Writing – original draft, Visualization. **Dominika Jakubczyk:** Methodology, Formal analysis, Investigation, Writing – original draft. **Corine Sandström:** Investigation, Writing – review & editing. **Dagmar Šrůtková:** Resources, Writing – review & editing. **Marcelina Joanna Pyclik:** Methodology, Investigation, Resources. **Katarzyna Leszczyńska:** Methodology, Resources. **Jarosław Ciekot:** Investigation. **Agnieszka Razim:** Methodology, Resources. **Martin Schwarzer:** Resources, Writing – review & editing, Supervision. **Sabina Górska:** Conceptualization, Validation, Writing – review & editing, Supervision, Project administration, Funding acquisition.

Declaration of competing interest

The authors declare no conflict of interest.

Data availability

Data will be made available on request.

Appendix A. Supplementary data

Supplementary data to this article can be found online at https://doi.org/10.1016/j.carbpol.2023.120980.

References

Altmann, F., Kosma, P., O'Callaghan, A., Leahy, S., Bottacini, F., Molloy, E., Plattner, S., Schiavi, E., Gleinser, M., Groeger, D., Grant, R., Rodriguez Perez, N., Healy, S., Svehla, E., Windwarder, M., Hofinger, A., O'Connell Motherway, M., Akdis, C. A., Xu, J.O'Mahony, L., … (2016). Genome analysis and characterisation of the exopolysaccharide produced by bifidobacterium longum subsp. Longum 35624TM. *PLOS ONE, 11*(9), Article e0162983. https://doi.org/10.1371/journal. pone.0162983

Amrouche, T., Boutin, Y., Prioult, G., & Fliss, I. (2006). Effects of bifidobacterial cytoplasm, cell wall and exopolysaccharide on mouse lymphocyte proliferation and cytokine production. *International Dairy Journal, 16*(1), 70–80. https://doi.org/ 10.1016/j.idairyj.2005.01.008

Balaguer, F., Enrique, M., Llopis, S., Barrena, M., Navarro, V., Álvarez, B., Chenoll, E., Ramón, D., Tortajada, M., & Martorell, P. (2022). Lipoteichoic acid from bifidobacterium animalis subsp. Lactis BPL1: A novel postbiotic that reduces fat deposition via IGF-1 pathway. *Microbial Biotechnology, 15*(3), 805–816. https://doi. org/10.1111/1751-7915.13769

Carillo, S., Silipo, A., Perino, V., Lanzetta, R., Parrilli, M., & Molinaro, A. (2009). The structure of the O-specific polysaccharide from the lipopolysaccharide of burkholderia anthina. *Carbohydrate Research, 344*(13), 1697–1700. https://doi.org/ 10.1016/j.carres.2009.05.013

Ciucanu, I., & Kerek, F. (1984). A simple and rapid method for the permethylation of carbohydrates. *Carbohydrate Research, 131*(2), 209–217. https://doi.org/10.1016/ 0008-6215(84)85242-8

Clarke, T. B., Davis, K. M., Lysenko, E. S., Zhou, A. Y., Yu, Y., & Weiser, J. N. (2010). Recognition of peptidoglycan from the microbiota by Nod1 enhances systemic innate immunity. *Nature Medicine, 16*(2), 228–231. https://doi.org/10.1038/nm.2087

Corridoni, D., Shiraishi, S., Chapman, T., Steevels, T., Muraro, D., Thézénas, M.-L., Prota, G., Chen, J.-L., Gileadi, U., Ternette, N., Cerundolo, V., & Simmons, A. (2019). NOD2 and TLR2 signal via TBK1 and PI31 to direct cross-presentation and CD8 T cell responses. *Frontiers in Immunology, 10*, 958. https://doi.org/10.3389/ fimmu.2019.00958

Dessing, M. C., Schouten, M., Draing, C., Levi, M., von Aulock, S., & van der Poll, T. (2008). Role played by toll-like receptors 2 and 4 in lipoteichoic acid-induced lung inflammation and coagulation. *The Journal of Infectious Diseases, 197*(2), 245–252. https://doi.org/10.1086/524873

DuBois, M., Gilles, K. A., Hamilton, J. K., Rebers, P. A., & Smith, F. (1956). Colorimetric method for determination of sugars and related substances. *Analytical Chemistry, 28* (3), 350–356. https://doi.org/10.1021/ac60111a017

Górska, S., Hermanova, P., Ciekot, J., Schwarzer, M., Srutkova, D., Brzozowska, E., Kozakova, H., & Gamian, A. (2016). Chemical characterization and immunomodulatory properties of polysaccharides isolated from probiotic lactobacillus casei LOCK 0919. *Glycobiology, 26*(9), 1014–1024. https://doi.org/ 10.1093/glycob/cww047

Górska, S., Jachymek, W., Rybka, J., Strus, M., Heczko, P. B., & Gamian, A. (2010). Structural and immunochemical studies of neutral exopolysaccharide produced by lactobacillus johnsonii 142. *Carbohydrate Research, 345*(1), 108–114. https://doi. org/10.1016/j.carres.2009.09.015

Górska, S., Schwarzer, M., Jachymek, W., Srutkova, D., Brzozowska, E., Kozakova, H., & Gamian, A. (2014). Distinct immunomodulation of bone marrow-derived dendritic cell responses to lactobacillus plantarum WCFS1 by two different polysaccharides isolated from lactobacillus rhamnosus LOCK 0900. *Applied and Environmental Microbiology, 80*(20), 6506–6516. https://doi.org/10.1128/AEM.02104-14

Górska, S., Schwarzer, M., Srutkova, D., Hermanova, P., Brzozowska, E., Kozakova, H., & Gamian, A. (2017). Polysaccharides L900/2 and L900/3 isolated from lactobacillus rhamnosus LOCK 0900 modulate allergic sensitization to ovalbumin in a mouse model. *Microbial Biotechnology, 10*(3), 586–593. https://doi.org/10.1111/1751-7915.12606

Hatano, S., Hirose, Y., Yamamoto, Y., Murosaki, S., & Yoshikai, Y. (2015). Scavenger receptor for lipoteichoic acid is involved in the potent ability of lactobacillus plantarum strain L-137 to stimulate production of interleukin-12p40. *International Immunopharmacology, 25*(2), 321–331. https://doi.org/10.1016/j. intimp.2015.02.011

Hiramatsu, Y., Hosono, A., Konno, T., Nakanishi, Y., Muto, M., Suyama, A., Hachimura, S., Sato, R., Takahashi, K., & Kaminogawa, S. (2011). Orally administered bifidobacterium triggers immune responses following capture by CD11c+ cells in Peyer's patches and cecal patches. *Cytotechnology, 63*(3), 307–317. https://doi.org/10.1007/s10616-011-9349-6

Hosono, A., Adachi, T., & Kaminogawa, S. (1977). (n.d.). In *Characterization of a water-soluble polysaccharide fraction with immunopotentiating activity from Bifidobacterium adolescentis MIOI-4* (p. 5).

Inturri, R., Molinaro, A., Di Lorenzo, F., Blandino, G., Tomasello, B., Hidalgo-Cantabrana, C., De Castro, C., & Ruas-Madiedo, P. (2017). Chemical and biological properties of the novel exopolysaccharide produced by a probiotic strain of bifidobacterium longum. *Carbohydrate Polymers, 174*, 1172–1180. https://doi.org/ 10.1016/j.carbpol.2017.07.039

Ivashkiv, L. B. (2018). IFNγ: Signalling, epigenetics and roles in immunity, metabolism, disease and cancer immunotherapy. *Nature Reviews Immunology, 18*(9), 545–558. https://doi.org/10.1038/s41577-018-0029-z

Jeong, J. H., Jang, S., Jung, B. J., Jang, K.-S., Kim, B.-G., Chung, D. K., & Kim, H. (2015). Differential immune-stimulatory effects of LTAs from different lactic acid bacteria via MAPK signaling pathway in RAW 264.7 cells. *Immunobiology, 220*(4), 460–466. https://doi.org/10.1016/j.imbio.2014.11.002

Kerry, R., George, Patra, J. K., Gouda, S., Park, Y., Shin, H.-S., & Das, G. (2018). Benefaction of probiotics for human health: A review. *Journal of Food and Drug Analysis, 26*(3), 927–939. https://doi.org/10.1016/j.jfda.2018.01.002

Kohno, M., Suzuki, S., Kanaya, T., Yoshino, T., Matsuura, Y., Asada, M., & Kitamura, S. (2009). Structural characterization of the extracellular polysaccharide produced by bifidobacterium longum JBL05. *Carbohydrate Polymers, 77*(2), 351–357. https://doi. org/10.1016/j.carbpol.2009.01.013

Laws, A., Gu, Y., & Marshall, V. (2001). Biosynthesis, characterisation, and design of bacterial exopolysaccharides from lactic acid bacteria. *Biotechnology Advances, 19* (8), 597–625. https://doi.org/10.1016/S0734-9750(01)00084-2

Li, A.-L., Sun, Y.-Q., Du, P., Meng, X.-C., Guo, L., Li, S., & Zhang, C. (2017). The effect of lactobacillus actobacillus peptidoglycan on bovine β-lactoglobulin-sensitized mice via TLR2/NF-κB pathway. *Iranian Journal of Allergy Asthma and Immunology, 16*(2), 147–158. PMID: 28601055.

Lipkind, G. M., Shashkov, A. S., Knirel, Y. A., Vinogradov, E. V., & Kochetkov, N. K. (1988). A computer-assisted structural analysis of regular polysaccharides on the basis of 13C-n.m.r. data. *Carbohydr. Res., 175*(1), 59–75. https://doi.org/10.1016/ 0008-6215(88)80156-3

Lu, Q., Guo, Y., Yang, G., Cui, L., Wu, Z., Zeng, X., Pan, D., & Cai, Z. (2022). Structure and anti-inflammation potential of lipoteichoic acids isolated from lactobacillus strains. *Foods, 11*(11), 1610. https://doi.org/10.3390/foods11111610

Martinic, M. M., Caminschi, I., O'Keeffe, M., Thinnes, T. C., Grumont, R., Gerondakis, S., McKay, D. B., Nemazee, D., & Gavin, A. L. (2017). The bacterial peptidoglycan-sensing molecules NOD1 and NOD2 promote CD8 + thymocyte selection. *The Journal of Immunology, 198*(7), 2649–2660. https://doi.org/10.4049/ jimmunol.1601462

Mattos, K. A., Jones, C., Heise, N., Previato, J. O., & Mendonça-Previato, L. (2001). Structure of an acidic exopolysaccharide produced by the diazotrophic endophytic bacterium burkholderia brasiliensis: Exopolysaccharide from nitrogen-fixing burkholderia. *European Journal of Biochemistry, 268*(11), 3174–3179. https://doi. org/10.1046/j.1432-1327.2001.02196.x

Morath, S., Geyer, A., & Hartung, T. (2001). Structure-function relationship of cytokine induction by lipoteichoic acid fromStaphylococcus aureus. *Journal of Experimental Medicine, 193*(3), 393–398. https://doi.org/10.1084/jem.193.3.393

Nagaoka, M., Hashimoto, S., Shibata, H., Kimura, I., Kimura, K., Sawada, H., & Yokokura, T. (1996). Structure of a galactan from cell walls of bifidobacterium catenulatum YIT4016. *Carbohydrate Research, 281*(2), 285–291. https://doi.org/ 10.1016/0008-6215(95)00354-1

Nagaoka, M., Muto, M., Yokokura, T., & Mutai, M. (1988). Structure of 6-deoxytalose-containing polysaccharide from the Cell Wall of bifidobacterium adolescentis. *The Journal of Biochemistry, 103*(4), 618–621. https://doi.org/10.1093/oxfordjournals. jbchem.a122316

Nataraj, B. H., Ali, S. A., Behare, P. V., & Yadav, H. (2020). Postbiotics-parabiotics: The new horizons in microbial biotherapy and functional foods. *Microbial Cell Factories, 19*(1), 168. https://doi.org/10.1186/s12934-020-01426-w

Palomares, O., Akdis, M., Martín-Fontecha, M., & Akdis, C. A. (2017). Mechanisms of immune regulation in allergic diseases: The role of regulatory T and B cells. *Immunological Reviews, 278*(1), 219–236. https://doi.org/10.1111/imr.12555

Pyclik, M. J., Srutkova, D., Razim, A., Hermanova, P., Svabova, T., Pacyga, K., Schwarzer, M., & Górska, S. (2021). Viability status-dependent effect of Bifidobacterium longum ssp. Longum CCM 7952 on prevention of allergic inflammation in mouse model. *Frontiers in Immunology, 12*, 2800. https://doi.org/ 10.3389/fimmu.2021.707728

Pyclik, M., Srutkova, D., Schwarzer, M., & Górska, S. (2020). Bifidobacteria cell wall-derived exo-polysaccharides, lipoteichoic acids, peptidoglycans, polar lipids and proteins – their chemical structure and biological attributes. *International Journal of Biological Macromolecules, 147*, 333–349. https://doi.org/10.1016/j. ijbiomac.2019.12.227

Raftis, E. J., Delday, M. I., Cowie, P., McCluskey, S. M., Singh, M. D., Ettorre, A., & Mulder, I. E. (2018). Bifidobacterium breve MRx0004 protects against airway inflammation in a severe asthma model by suppressing both neutrophil and eosinophil lung infiltration. *Scientific Reports, 8*(1), 12024. https://doi.org/10.1038/ s41598-018-30448-z

Robinson, D. S., Larché, M., & Durham, S. R. (2004). Tregs and allergic disease. *Journal of Clinical Investigation, 114*(10), 1389–1397. https://doi.org/10.1172/JCI200423595

Ruiz, L., Delgado, S., Ruas-Madiedo, P., Sánchez, B., & Margolles, A. (2017). Bifidobacteria and their molecular communication with the immune system. *Frontiers in Microbiology, 8*, 2345. https://doi.org/10.3389/fmicb.2017.02345

Salatin, S., & Yari Khosroushahi, A. (2017). Overviews on the cellular uptake mechanism of polysaccharide colloidal nanoparticles. *Journal of Cellular and Molecular Medicine, 21*(9), 1668–1686. https://doi.org/10.1111/jcmm.13110

Sawardeker, J. S., Sloneker, J. H., & Jeanes, A. (1965). Quantitative determination of monosaccharides as their alditol acetates by gas liquid chromatography. *Analytical Chemistry, 37*(12), 1602–1604. https://doi.org/10.1021/ac60231a048

Schaub, R., & Dillard, J. (2017). Digestion of peptidoglycan and analysis of soluble fragments. *BIO-Protocol, 7*(15). https://doi.org/10.21769/BioProtoc.2438

Schiavi, E., Gleinser, M., Molloy, E., Groeger, D., Frei, R., Ferstl, R., Rodriguez-Perez, N., Ziegler, M., Grant, R., Moriarty, T. F., Plattner, S., Healy, S., O'Connell Motherway, M., Akdis, C. A., Roper, J., Altmann, F., van Sinderen, D., & O'Mahony, L. (2016). The surface-associated exopolysaccharide of bifidobacterium longum 35624 plays an essential role in dampening host proinflammatory responses and repressing local T H 17 responses. *Applied and Environmental Microbiology, 82* (24), 7185–7196. https://doi.org/10.1128/AEM.02238-16

Schiavi, E., Plattner, S., Rodriguez-Perez, N., Barcik, W., Frei, R., Ferstl, R., Kurnik-Lucka, M., Groeger, D., Grant, R., Roper, J., Altmann, F., van Sinderen, D., Akdis, C. A., & O'Mahony, L. (2018). Exopolysaccharide from bifidobacterium

longum subsp. Longum 35624TM modulates murine allergic airway responses. *Beneficial Microbes, 9*(5), 761–773. https://doi.org/10.3920/BM2017.0180

Schröder, N. W. J., Morath, S., Alexander, C., Hamann, L., Hartung, T., Zähringer, U., Göbel, U. B., Weber, J. R., & Schumann, R. R. (2003). Lipoteichoic acid (LTA) of streptococcus pneumoniaeand Staphylococcus aureus activates immune cells via toll-like receptor (TLR)-2, lipopolysaccharide-binding protein (LBP), and CD14, whereas TLR-4 and MD-2 are not involved. *Journal of Biological Chemistry, 278*(18), 15587–15594. https://doi.org/10.1074/jbc.M212829200

Schwarzer, M., Srutkova, D., Schabussova, I., Hudcovic, T., Akgün, J., Wiedermann, U., & Kozakova, H. (2013). Neonatal colonization of germ-free mice with bifidobacterium longum prevents allergic sensitization to major birch pollen allergen bet v 1. *Vaccine, 31*(46), 5405–5412. https://doi.org/10.1016/j.vaccine.2013.09.014

Senchenkova, S. N., Shashkov, A. S., Laux, P., Knirel, Y. A., & Rudolph, K. (1999). The O-chain polysaccharide of the lipopolysaccharide of xanthomonascampestris pv. Begoniae GSPB 525 is a partially l-xylosylated l-rhamnan. *Carbohydrate Research, 319*(1–4), 148–153. https://doi.org/10.1016/S0008-6215(99)00125-1

Shang, N., Xu, R., & Li, P. (2013). Structure characterization of an exopolysaccharide produced by bifidobacterium animalis RH. *Carbohydrate Polymers, 91*(1), 128–134. https://doi.org/10.1016/j.carbpol.2012.08.012

Shashkov, A. S., Lipkind, G. M., Knirel, Y. A., & Kochetkov, N. K. (1988). Stereochemical factors determining the effects of glycosylation on the13C chemical shifts in carbohydrates. *Magnetic Resonance in Chemistry, 26*(9), 735–747. https://doi.org/10.1002/mrc.1260260904

Speciale, I., Verma, R., Di Lorenzo, F., Molinaro, A., Im, S.-H., & De Castro, C. (2019). Bifidobacterium bifidum presents on the cell surface a complex mixture of glucans and galactans with different immunological properties. *Carbohydrate Polymers, 218*, 269–278. https://doi.org/10.1016/j.carbpol.2019.05.006

Tejada-Simon, M. V., & Pestka, J. J. (1999). Proinflammatory cytokine and nitric oxide induction in murine macrophages by Cell Wall and cytoplasmic extracts of lactic acid bacteria. *Journal of Food Protection, 62*(12), 1435–1444. https://doi.org/10.4315/0362-028X-62.12.1435

Tian, X., Fan, R., He, H., Cui, Q., Liang, X., Liu, Q., Liu, T., Lin, K., Zhang, Z., Yi, H., Gong, P., & Zhang, L. (2022). Bifidobacterium animalis KV9 and lactobacillus

vaginalis FN3 alleviated β-lactoglobulin-induced allergy by modulating dendritic cells in mice. *Frontiers in Immunology, 13*, Article 992605. https://doi.org/10.3389/fimmu.2022.992605

Verma, R., Lee, C., Jeun, E.-J., Yi, J., Kim, K. S., Ghosh, A., Byun, S., Lee, C.-G., Kang, H.-J., Kim, G.-C., Jun, C.-D., Jan, G., Suh, C.-H., Jung, J.-Y., Sprent, J., Rudra, D., De Castro, C., Molinaro, A., Surh, C. D., & Im, S.-H. (2018). Cell surface polysaccharides of bifidobacterium bifidum induce the generation of Foxp3 + regulatory T cells. *Science Immunology, 3*(28), Article eaat6975. https://doi.org/10.1126/sciimmunol.aat6975

Vinogradov, E., Korenevsky, A., & Beveridge, T. J. (2003). The structure of the O-specific polysaccharide chain of the shewanella algae BrY lipopolysaccharide. *Carbohydrate Research, 338*(4), 385–388. https://doi.org/10.1016/S0008-6215(02)00469-X

Wolf, A. J., & Underhill, D. M. (2018). Peptidoglycan recognition by the innate immune system. *Nature Reviews Immunology, 18*(4), 243–254. https://doi.org/10.1038/nri.2017.136

Xu, R., Shen, Q., Wu, R., & Li, P. (2017). Structural analysis and mucosal immune regulation of exopolysaccharide fraction from bifidobacterium animalis RH. *Food and Agricultural Immunology, 28*(6), 1226–1241. https://doi.org/10.1080/09540105.2017.1333578

Zdorovenko, E. L., Kachala, V. V., Sidarenka, A. V., Izhik, A. V., Kisileva, E. P., Shashkov, A. S., Novik, G. I., & Knirel, Y. A. (2009). Structure of the cell wall polysaccharides of probiotic bifidobacteria bifidobacteriumbifidum BIM B-465. *Carbohydrate Research, 344*(17), 2417–2420. https://doi.org/10.1016/j.carres.2009.08.039

Zeuthen, L. H., Fink, L. N., & Frøkiaer, H. (2008). Toll-like receptor 2 and nucleotide-binding oligomerization domain-2 play divergent roles in the recognition of gut-derived lactobacilli and bifidobacteria in dendritic cells. *Immunology, 124*(4), 489–502. https://doi.org/10.1111/j.1365-2567.2007.02800.x

Zhou, Y., Cui, Y., & Qu, X. (2019). Exopolysaccharides of lactic acid bacteria: Structure, bioactivity and associations: A review. *Carbohydrate Polymers, 207*, 317–332. https://doi.org/10.1016/j.carbpol.2018.11.093